

# Cobalt-based nanocatalyst catalyzed one-pot four-component synthesis 2*H*-indazolo[2,1-*b*]phthalazine-triones under solvent-free condition

Jalal Albadi<sup>1</sup> · Mehdi Jalali<sup>2</sup> · Ahmadreza Momeni<sup>1</sup>

Received: 7 November 2017 / Accepted: 11 December 2017 / Published online: 27 December 2017  
© Springer Science+Business Media B.V., part of Springer Nature 2017

**Abstract** In this research, an efficient procedure for the one-pot four-component synthesis of 2*H*-indazolo[2,1-*b*]phthalazine-triones catalyzed by a cobalt-based nanocatalyst (Co/Al<sub>2</sub>O<sub>3</sub> nanocatalyst) is reported. The catalyst was prepared by a co-precipitation method and characterized by BET surface area, SEM, TEM, EDS and XRD analyses. A wide range of various aromatic aldehydes including electron-withdrawing and electron-releasing groups were applied and corresponding products obtained in high yields without any by-product. Moreover, the Co/Al<sub>2</sub>O<sub>3</sub> is recyclable up to 7 consecutive runs by simple filtration.

**Keywords** Co/Al<sub>2</sub>O<sub>3</sub> nanocatalyst · 2*H*-indazolo[2,1-*b*]phthalazine-triones · Four-component synthesis · Solvent-free condition

## Introduction

Phthalazine derivatives are an important class of heterocyclic compounds that has received significant attention from many organic and pharmaceutical chemists due to their broad biological and pharmacological activities such as anticonvulsant, cardiotoxic, and vasorelaxant [1, 2]. Phthalazines have been found to be effective for the inhibition of p38 MAP kinase, for selective binding of GABA receptor, and an

---

**Electronic supplementary material** The online version of this article (<https://doi.org/10.1007/s11164-017-3236-5>) contains supplementary material, which is available to authorized users.

---

✉ Jalal Albadi  
chemalbadi@gmail.com; albadi@sci.sku.ac.ir

<sup>1</sup> Department of Chemistry, Faculty of Science, Shahrekord University, Shahrekord, Iran

<sup>2</sup> National Petrochemical Company, Petrochemical Research and Technology Company, Tehran, Iran

as anti-anxiety drug and antitumor agent [3, 4]. Moreover, these compounds show unique electrical and optical properties [5].

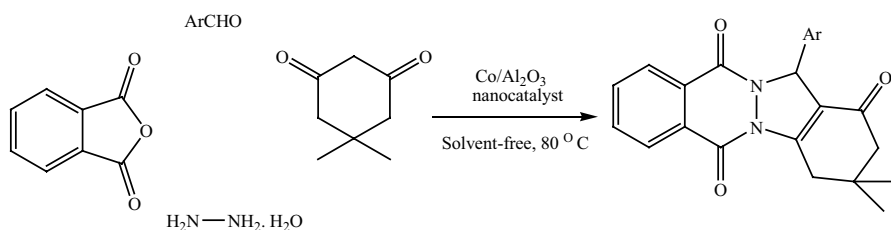
Various synthetic procedures for the synthesis of 2*H*-indazolo[2,1-*b*]phthalazine-triones involving three-component reaction of aldehydes, 1,3-dicarbonyl compounds (dimedone or cyclohexane-1,3-dione) with 2,3-dihydro-1,4-phthalazinedione (phthalhydrazide) and/or one-pot four-component reactions between aldehydes, 1,3-dicarbonyl compounds (dimedone or cyclohexane-1,3-dione), hydrazinium hydroxide and phthalic anhydride have been reported [6–21].

Alumina-supported cobalt catalysts are an important material system in the field of heterogeneous catalysis. It has been reported that metal–support interactions may considerably affect the surface properties and hence catalytic activity [22, 23]. Among these catalysts, Co/Al<sub>2</sub>O<sub>3</sub> catalysts have been studied in various processes several times over the years especially for their activity in CO hydrogenation [24–26]. However, to the best of our knowledge, the performance of Co/Al<sub>2</sub>O<sub>3</sub> nanocatalysts as Lewis acids has not investigated over organic synthesis reactions especially for the synthesis of 2*H*-indazolo[2,1-*b*]phthalazine-triones.

On the other hand, recently, the practical applications of supported-metallic nanoparticles as the catalysts in organic synthesis have increased due to good activation of adsorbed compounds, reaction rate improvement, easier work-up, recyclability and the eco-friendly reaction conditions. Therefore, in continuation of our studies on the catalytic activity of different nanocatalysts on the organic reactions [27–33], here, we wish to report the performance of a cobalt-based nanocatalyst (Co/Al<sub>2</sub>O<sub>3</sub> nanocatalyst) as an efficient recyclable catalyst in the synthesis of 2*H*-indazolo[2,1-*b*]phthalazine-triones under solvent-free conditions (Scheme 1).

## Experimental

Products were characterized by comparison of their spectroscopic data (NMR and IR) and physical properties with those reported in the literature. The NMR spectra were recorded on a Bruker Advance 400 MHz. IR spectra were recorded on a Perkin Elmer 781 Spectrophotometer. Yields refer to isolated pure products. The XRD analysis was performed using an X-ray diffractometer, Cu-K $\alpha$  monochromatized radiation source and a nickel filter (PANalytical X'Pert-Pro) in order to investigate the



**Scheme 1** Four-component synthesis of 2*H*-indazolo[2,1-*b*]phthalazine-triones catalyzed by Co/Al<sub>2</sub>O<sub>3</sub> nanocatalyst

structure and crystallinity of the catalyst. The Scherrer equation was used to establish the average crystallite size of the sample. A flame atomic absorption spectrophotometer (GBC 906AA) was applied to determine the amount of cobalt content of the catalyst. The BET surface area of the catalyst was tested by the  $N_2$  adsorption–desorption method. The analysis were carried out using an automated gas adsorption analyzer (Tristar 3020; Micromeritics). The sample was purged with nitrogen gas for 3 h at 300 °C by a VacPrep 061 degas system (Micromeritics). The morphology of the prepared catalyst was analyzed by scanning electron microscopy (SEM) using a JEOL JSM-6500F instrument, equipped with an EDS analytical system to study the presence of different components of the catalyst. Transmission electron microscopy (TEM) analysis was also performed using a JEOL JEM-2100 (200 kV) microscope equipped with an EDS analytical system. The size of about 200 cobalt nanoparticles were measured in order to determine their distribution and average particle size.

### Catalyst preparation

The  $Co/Al_2O_3$  nanocatalyst was prepared by a co-precipitation process. An aqueous solution of 0.5 M NaOH was added into a mixture of 0.5 M cobalt nitrate and aluminium nitrate under vigorous stirring at 50 °C. The obtained solution was aged at pH of 9 for 1 h, then filtered and washed with deionized water to remove the interfering ions. The sample was dried overnight at 100 °C and then calcined in air at 450 °C for 4 h. Also, a batch of the  $Al_2O_3$  support without Co content was prepared by the same method for the supplementary analysis.

### General procedure for the synthesis of 2*H*-indazolo[2,1-*b*]phthalazine-triones

A mixture of dimedone (1 mmol), aromatic aldehyde (1 mmol), hydrazinium hydroxide (1.2 mmol) and phthalic anhydride (1 mmol) in the presence of  $Co/Al_2O_3$  nanocatalyst (0.05 g), heated in an oil bath at 100 °C for appropriate times. After reaction completion (monitored by TLC), the mixture was cooled to room temperature, hot ethanol was added and the catalyst was separated. Evaporation of the solvent from the resulting solution and recrystallization of the solid residue from hot ethanol afforded the pure products in high yields.

## Results and discussion

### Catalyst characterization results

From XRD analysis (Fig. 1), the  $Co/Al_2O_3$  nanocatalyst shows diffraction peaks at  $2\theta = 37.60^\circ$ ,  $45.79^\circ$ ,  $66.76^\circ$  and  $85.02^\circ$ , which are attributed to the [110], [111], [211] and [300] planes, respectively, of  $\gamma-Al_2O_3$  [code No. 01-1303]. The diffraction peaks at  $19.04^\circ$ ,  $31.35^\circ$ ,  $36.94^\circ$ ,  $44.92^\circ$ ,  $59.51^\circ$ ,  $65.41^\circ$  and  $77.56^\circ$  respectively correspond to [111], [220], [311], [400], [511], [440] and [533] planes of cubic  $Co_3O_4$  (code No. 01-074-1657). Moreover, the XRD pattern of the cobalt nanocatalyst

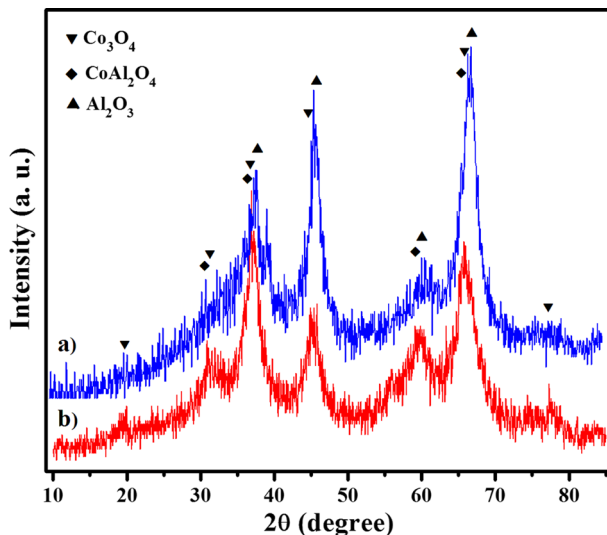


**Fig. 1** XRD pattern of the cobalt nanocatalyst and the  $\text{Al}_2\text{O}_3$  support

shows a distinct peak at  $94.38^\circ$  which is attributed to the [731] plane of  $\text{CoAl}_2\text{O}_4$  (code No. 03-0896). This peak indicates the incorporation of Co species into the structure of the  $\text{Al}_2\text{O}_3$  support at calcination temperatures as high as  $450^\circ\text{C}$ . The average crystallite size of Co oxide in the  $\text{Co}/\text{Al}_2\text{O}_3$  nanocatalyst, calculated by the Debye–Scherrer equation, is about 11.1 nm.

Table 1 shows the structural properties of the samples. The amount of Co content in the catalyst analyzed by atomic absorption spectroscopy is 9.6 wt%. The alumina support has a high BET surface area of about  $270\text{ m}^2\text{ g}^{-1}$ ; however, after incorporation of Co content, the BET is decreased to about  $252\text{ m}^2\text{ g}^{-1}$ .

Figure 2 shows the  $\text{N}_2$  adsorption/desorption profiles of the catalysts. The results show that the alumina support and the Co nanocatalyst exhibit adsorption/desorption isotherm profiles with hysteresis loops between  $p/p^0 = 0.45\text{--}0.9$ . Based upon the IUPAC classification, this type of isotherm is categorized as type IV, and ascribed to mesoporous structures. While the alumina support adsorption profile shows a H3 type hysteresis loop, which can demonstrate

**Table 1** Structural properties of the  $\text{Al}_2\text{O}_3$  support and  $\text{Co}/\text{Al}_2\text{O}_3$  nanocatalyst

Sample	Co content <sup>a</sup> (wt%)	Co crystallite size <sup>b</sup> (nm)	BET surface area ( $\text{m}^2\text{ g}^{-1}$ )	Avg. pore size (nm)	Pore volume ( $\text{cm}^3\text{ g}^{-1}$ )
$\text{Al}_2\text{O}_3$	0.0	–	269	2.8	0.21
$\text{Co}/\text{Al}_2\text{O}_3$	9.6	11.1	252	4.0	0.24

<sup>a</sup>Measured by atomic absorption method

<sup>b</sup>Average Co crystallite size calculated by XRD

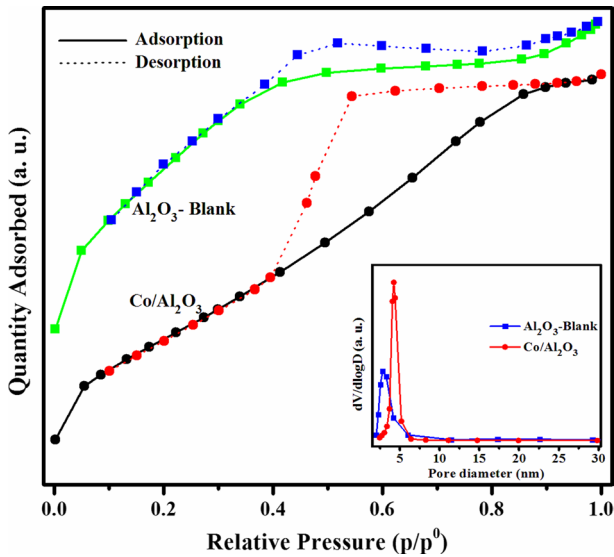


**Fig. 2**  $N_2$  adsorption/desorption profiles of the  $Co/Al_2O_3$  nanocatalyst

aggregates of nonuniform narrow slit-like pores of plate-like and/or cubic nanoparticles, the  $Co/Al_2O_3$  sample shows a H2 hysteresis loop which is common for mesoporous carriers and catalysts. This type of hysteresis loop is attributed to aggregates and agglomerates of spheroidal particles with nonuniform sized and shaped pores [34, 35]. As exhibited in Fig. 2, the alumina support and the cobalt nanocatalyst display narrow pore size distributions with a maximum at 3 and 4 nm, respectively.

Figure 3 displays the SEM images and the EDS results of the  $Co/Al_2O_3$  nanocatalyst. The SEM analysis shows a uniform aggregation of nanoparticles with a diameter of about 21 nm. This result is in accordance with the type IV hysteresis H2 isotherm shown by the  $N_2$  adsorption/desorption test.

As shown in Fig. 3, cobalt nanoparticles are dispersed on the alumina support with a particle size distribution between 3 and 13 nm, and an average size of about 6.5 nm. The HRTEM image of the catalyst (Fig. 4) exhibits reflections with  $d$ -spacing values of about 0.24 nm which correspond to the  $Co_3O_4$  (311) lattice plane.

The EDS analysis shows a cobalt content of about 15.4 wt% on the surface of the catalyst. The higher Co loading in comparison to the nominal Co loading (10 wt%) could be due to the procedure of the synthesis of the catalyst. By considering the higher  $K_{sp}$  number of  $Co(OH)_2$ ,  $3 \times 10^{-16}$ , in comparison to the  $K_{sp}$  of  $Al(OH)_3$ ,  $3 \times 10^{-34}$ , it can be suggested that, with a gradual increase of the pH of solution during the co-precipitation procedure, the Co clusters tend to precipitate at higher pH values, which results in an increase in the amount of Co content on the surface of the  $Co/Al_2O_3$  nanocatalyst.

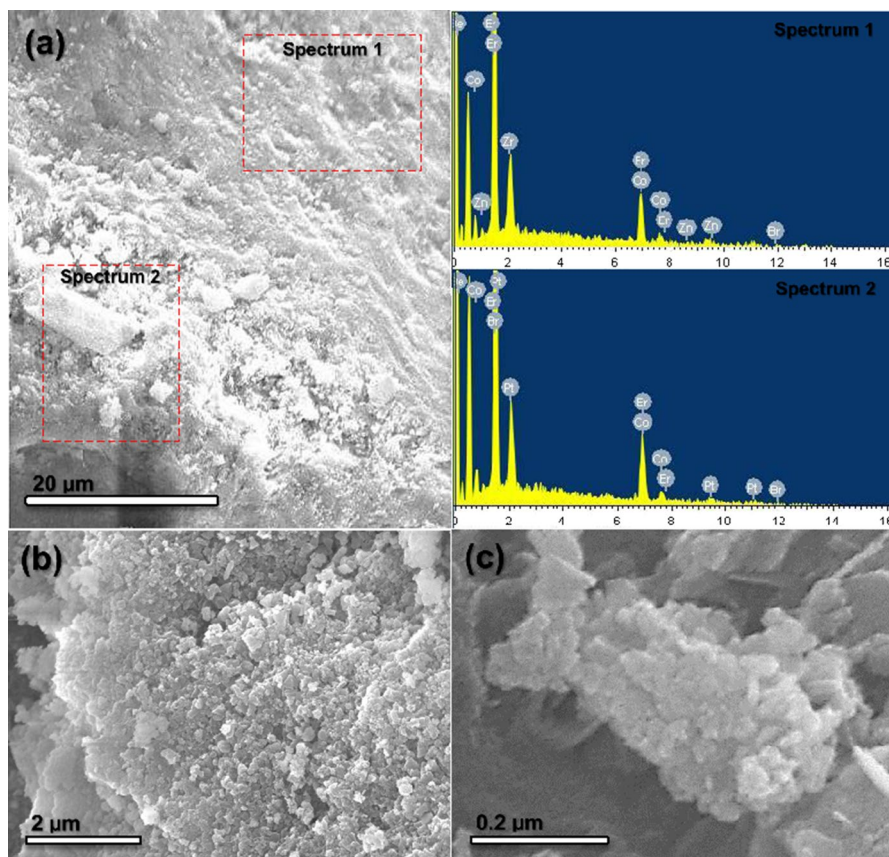


**Fig. 3** SEM images and EDS analysis results of the Co/Al<sub>2</sub>O<sub>3</sub> nanocatalyst

### Catalytic performance

To find the best reaction conditions, the one-pot four-component reaction of benzaldehyde with hydrazinium hydroxide, phthalic anhydride and dimedone was selected as a model and its behavior was studied under a variety of conditions. Several reaction conditions were examined and the yield and reaction times were monitored in the presence of different amounts of Co/Al<sub>2</sub>O<sub>3</sub> nanocatalyst.

The obtained results are summarized in Table 2. To study the effect of reaction temperature, the reaction was carried out at different temperatures. At room temperature, the reaction rate was found to be slow, and it was improved at higher temperatures. The best result was found at 80 °C, and further increases in temperature did not show any improvement. The model reaction was studied in the presence of different amounts of Co/Al<sub>2</sub>O<sub>3</sub> nanocatalyst. It was found that using 0.05 g of the Co/Al<sub>2</sub>O<sub>3</sub> nanocatalyst was sufficient for the reaction to complete. When the amount of the catalyst was lower, the time increased and the yield of the product reduced.

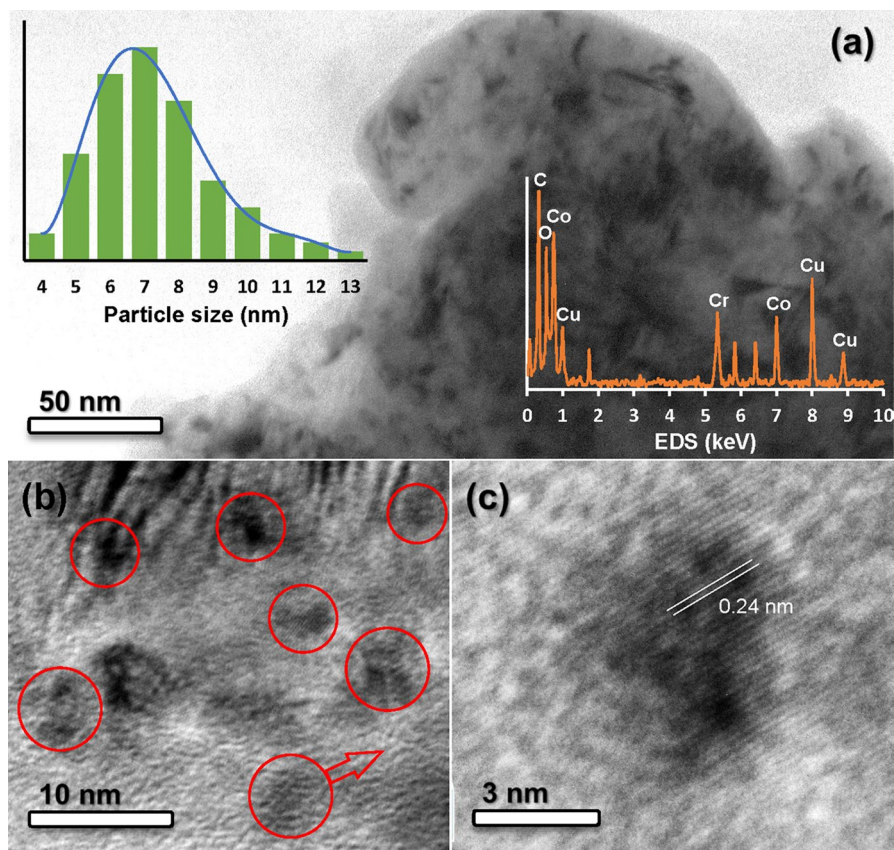


**Fig. 4** TEM image of Co/Al<sub>2</sub>O<sub>3</sub> nanocatalyst. Particle size distribution of Co and EDS analysis results of the catalyst (a), dispersion and size of Co nanoparticles (b), and HRTEM image of the catalyst (c)

Moreover, various solvents were examined and solvent-free conditions were found to be the most optimum in terms of yield of product and reaction rate. Consequently, the best result was achieved by carrying out the reaction in the presence of 0.05 g of the Co/Al<sub>2</sub>O<sub>3</sub> nanocatalyst under solvent-free condition at 80 °C.

In the next step, the extent and efficiency of this process was investigated under the optimized reaction conditions. Therefore, a various range of aromatic aldehydes were condensed with phthalic anhydride, hydrazinium hydroxide and dimedone in the presence of the Co/Al<sub>2</sub>O<sub>3</sub> nanocatalyst under solvent-free condition.

As shown in Table 3, aromatic aldehydes having electron-withdrawing groups reacted at a faster rate compared with aromatic aldehydes substituted with electron-donating groups. All substrates were efficiently converted to their corresponding products in high yields and short reaction times without the formation of any by-product. The corresponding products were isolated by simple filtration and easily recrystallized in hot ethanol. Moreover, the products were

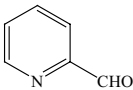
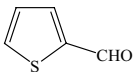
**Table 2** Optimization of the reaction conditions

Entry	Conditions <sup>a</sup>	Catalyst amounts (g)	Time (min)	Yield (%)
1	H <sub>2</sub> O/r.t.	0.03	600	Trace
2	H <sub>2</sub> O/reflux	0.03	600	25
3	H <sub>2</sub> O/reflux	0.05	600	45
4	EtOH/r.t.	0.03	600	Trace
5	EtOH/reflux	0.03	600	Trace
6	EtOH/reflux	0.05	600	30
7	CH <sub>3</sub> CN/reflux	0.05	600	Trace
8	CH <sub>3</sub> OH/reflux	0.05	600	Trace
9	Solvent-free/60 °C	0.03	60	40
10	Solvent-free/60 °C	0.05	35	70
11	Solvent-free/80 °C	0.03	30	70
12	Solvent-free/100 °C	0.05	12	93

Reaction conditions: benzaldehyde (1 mmol), hydrazinium hydroxide (1.2 mmol), phthalic anhydride (1 mmol), dimedone (1 mmol), under solvent-free condition

<sup>a</sup>Yield refers to isolated pure products

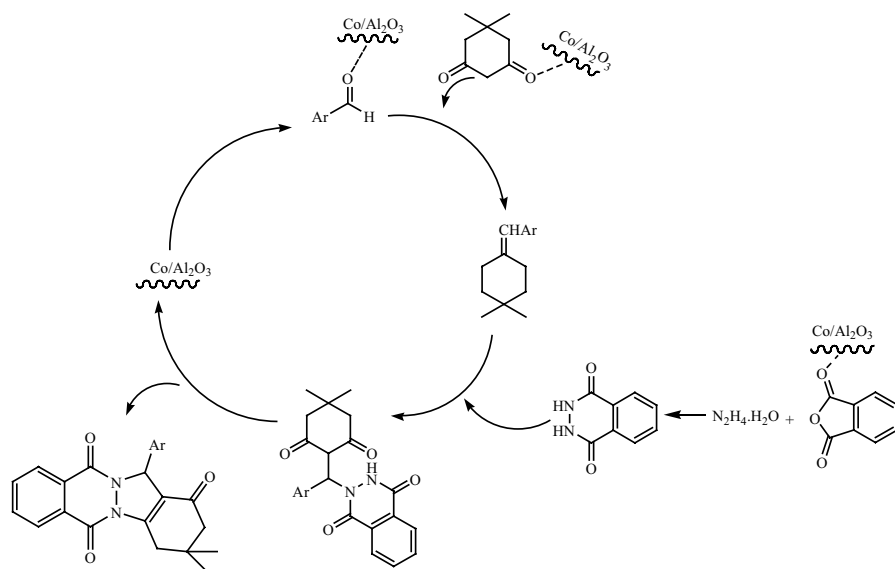
**Table 3** Synthesis of of 2*H*-indazolo[2,1-*b*]phthalazine-triones catalyzed by Co/Al<sub>2</sub>O<sub>3</sub> nanocatalyst

Entry	Aldehyde	Time (min)	Yield (%) <sup>a</sup>	M.P. (°C) <sup>b</sup>
1	C <sub>6</sub> H <sub>5</sub> CHO	12	93	205–207
2	4-ClC <sub>6</sub> H <sub>5</sub> CHO	10	93	261–263
3	3-ClC <sub>6</sub> H <sub>5</sub> CHO	12	92	209–211
4	2-ClC <sub>6</sub> H <sub>4</sub> CHO	12	91	262–264
5	2,4-Cl <sub>2</sub> C <sub>6</sub> H <sub>3</sub> CHO	10	93	220–222
6	4-NO <sub>2</sub> C <sub>6</sub> H <sub>4</sub> CHO	7	94	222–224
7	3-NO <sub>2</sub> C <sub>6</sub> H <sub>4</sub> CHO	15	92	272–274
8	2-MeC <sub>6</sub> H <sub>4</sub> CHO	12	92	240–242
9	4-MeC <sub>6</sub> H <sub>4</sub> CHO	17	91	228–230
10	4-MeOC <sub>6</sub> H <sub>4</sub> CHO	25	91	218–220
11	3-OHC <sub>6</sub> H <sub>4</sub> CHO	25	90	268–270
12	4-BrC <sub>6</sub> H <sub>4</sub> CHO	10	93	261–263
13	4-MeSC <sub>6</sub> H <sub>4</sub> CHO	22	92	228–230
14		20	89	229–231
15		25	88	241–243

<sup>a</sup>Isolated pure products

<sup>b</sup>Products were characterized by comparison of their spectroscopic data and melting points with those reported in the literature [12–21]





**Scheme 2** The proposed mechanism for the four-component synthesis of 2H-indazolo[2,1-b]phthalazine-triones catalyzed by the Co/Al<sub>2</sub>O<sub>3</sub> nanocatalyst

**Table 4** Recyclability study of Co/Al<sub>2</sub>O<sub>3</sub> nanocatalyst

Run	1	2	3	4	5	6	7
Time (min)	12	12	15	15	20	25	30
Yield (%) <sup>a</sup>	93	92	92	90	90	90	89

<sup>a</sup>Isolated yield

characterized by spectroscopic data (<sup>1</sup>HNMR, <sup>13</sup>CNMR and IR) and by comparison with the spectral data reported in the literature. A plausible mechanism of the reaction is shown in Scheme 2, with the reaction occurring via initial formation of the phthalhydrazide by nucleophilic addition of hydrazinium hydroxide to phthalic anhydride activated (by the Co/Al<sub>2</sub>O<sub>3</sub> nanocatalyst, followed by dehydration. The second step involves Knoevenagel condensation between dimedone and aldehyde activated by the Co/Al<sub>2</sub>O<sub>3</sub> nanocatalyst. Subsequent Michael-type addition of the phthalhydrazide followed by cyclization affords the corresponding product.

To investigate the recyclability of the catalyst, the reaction of benzaldehyde, dimedone, phthalic anhydride, and hydrazinium hydroxide under solvent-free conditions at 80 °C was studied. After reaction completion, the catalyst was washed with hot ethanol, dried and stored for another consecutive reaction run. The recovered catalyst was reused 7 times without any significant loss of activity (Table 4).

## Conclusion

In conclusion, an efficient cobalt-based nanocatalyst (Co/Al<sub>2</sub>O<sub>3</sub> nanocatalyst) was prepared, characterized and used for the one-pot four-component synthesis of 2*H*-indazolo[2,1-*b*]phthalazine-triones under solvent-free condition. The catalyst is stable and easily synthesized. It can promote the yields and reaction times over 7 runs with comparable activity. Moreover, heterogeneous reaction conditions, operational simplicity, enhanced rates and high isolated yields of pure products are major advantages will make this procedure a useful addition to the available methods.

**Acknowledgements** We are grateful to the Shahrekord University for the support of this work.

## References

1. F.W. Lichtenthaler, *Acc. Chem. Res.* **35**, 728 (2002)
2. V.P. Litvinov, *Russ. Chem. Rev.* **72**, 69 (2003)
3. J.S. Kim, H.J. Lee, M.E. Suh, H.Y.P. Choo, S.K. Lee, H.J. Park, C. Kim, S.W. Park, C.O. Lee, *Bioorg. Med. Chem.* **12**, 368 (2004)
4. Y. Imamura, A. Noda, T. Imamura, Y. Ono, T. Okawara, H. Noda, *Life Sci.* **74**, 29 (2003)
5. Y. Xu, Q.X. Guo, *Heterocycles* **63**, 903 (2004)
6. H.R. Shaterian, F. Rigi, *Res. Chem. Intermed.* **40**, 1989 (2014)
7. M.V. Reddy, G.C.S. Reddy, Y.T. Jeong, *Tetrahedron* **68**, 6820 (2012)
8. R. Tayebee, M. Fattahi Abdizadeh, B. Maleki, E. Shahri, *J. Mol. Liq.* **241**, 447 (2017)
9. A. Hashemzadeh, M.M. Amini, R. Tayebee, A. Sadeghian, L.J. Durndell, M.A. Isaacs, A. Osatiash-tiani, C.M.A. Parlett, A.F. Lee, *Mol. Catal.* **440**, 96 (2017)
10. A.V. Chate, P.K. Bhadke, M.A. Khande, J.N. Sangshetti, C.H. Gill, *Chin. Chem.* **28**, 1577 (2017)
11. M. Abedini, F. Shirini, J.M.A. Omran, *J. Mol. Liq.* **212**, 405 (2015)
12. E. Mosaddegh, A. Hassankhani, *Catal. Commun.* **71**, 65 (2015)
13. F. Shirini, M.S.N. Langarudi, O. Goli-Jolodar, *Dys Pig.* **123**, 186 (2015)
14. A.B. Atar, S.D. Lee, B.G. Cho, D.W. Cho, Y.T. Jeong, *Res. Chem. Intermed.* **42**, 1707 (2016)
15. E. Mosaddegh, A. Hassankhani, *Tetrahedron Lett.* **52**, 488 (2011)
16. A. Hasaninejed, M. Rasekhi Kazerooni, A. Zare, *Catal. Today* **196**, 148 (2012)
17. B. Atashkar, A. Rostami, H. Golami, B. Tahmasbi, *Res. Chem. Intermed.* **41**, 3675 (2015)
18. H.-J. Wang, X.N. Zhang, Z.H. Zhang, *Monatshfte Chem.* **141**, 425 (2010)
19. M. Esmailpour, J. Javidi, F. Dehghani, *J. Iran. Chem. Soc.* **13**, 655 (2016)
20. X.-N. Zhao, G.-F. Hu, M. Tang, T.-T. Shi, X.-L. Guo, T.-T. Li, Z.-H. Zhang, *RSC Adv.* **4**, 51089 (2014)
21. B. Dam, M. Saha, R. Jamatia, A.K. Pal, *RSC Adv.* **6**, 54768 (2016)
22. L. Ji, J. Lin, H.C. Zeng, *J. Phys. Chem. B.* **104**, 1783 (2000)
23. E. Iglesia, *Appl. Catal. A Gen.* **161**, 59 (1997)
24. S. Storsaeter, Ø. Borg, E.A. Blekkan, B. Tødal, A. Holmen, *Catal. Today* **100**, 343 (2005)
25. M. Lu, N. Fatah, A.Y. Khodakov, Y. Gu, *Green Chem.* **14**, 2091 (2012)
26. J. Zhang, J. Chen, J. Ren, Y. Li, Y. Sun, *Fuel* **82**, 581 (2003)
27. J. Albadi, A. Alihoseinzadeh, A. Razeghi, *Catal. Commun.* **49**, 1 (2014)
28. J. Albadi, A. Alihoseinzadeh, M. Jalali, M. Shahrezaei, A. Mansournezhad, *Mol. Catal.* **440**, 133 (2017)
29. J. Albadi, A. Mansournezhad, S. Salehnasab, *Res. Chem. Intermed.* **41**, 5713 (2015)
30. J. Albadi, J. Abbasi Shiran, A. Mansournezhad, *J. Chem. Sci.* **126**, 147 (2014)
31. J. Albadi, M. Keshavarz, F. Shirini, M. Vafaie-nezhad, *Catal. Commun.* **27**, 17 (2012)
32. J. Albadi, A. Mansournezhad, T. Sadeghi, *Res. Chem. Intermed.* **41**, 8317 (2015)
33. J. Albadi, A. Mansournezhad, *Res. Chem. Intermed.* **42**, 5739 (2016)
34. R.A. Sheldon, *Catal. Today* **1**, 351 (1987)
35. G. Leofanti, M. Padovan, G. Tozzola, B. Venturelli, *Catal. Today* **41**, 207 (1998)